

# Confinement modes and magnetic-island driven modes in the TJ-II stellarator

D. López-Bruna, B. J. Sun, M. A. Ochando, M. A. Pedrosa and the TJ-II Team

Laboratorio Nacional de Fusión, CIEMAT, Avda. Complutense 40, 28040 Madrid, Spain

*Corresponding Author:* daniel.lopezbruna@ciemat.es

## Abstract:

In the low magnetic shear plasmas of the stellarator TJ-II, magneto-hydrodynamic phenomena accompany the repetitive formation and destruction of transport barriers near magnetically resonant locations [Nuclear Fusion (2013) **53** 073051]. These processes are now related with the plasma response to vacuum magnetic islands: The islands are dragged by the ExB flow provoking quasi-coherent magnetic fluctuations that are intense during L-mode but significantly dimmed in H-mode; but when a barrier forms, an MHD instability can make the barrier collapse originating transport bursts that propagate out. An added drift of the islands with the electron diamagnetic speed seems to happen during the gradient relaxation until the barrier forms again, which causes a cyclic behaviour and a confinement quality that depends on the strength and repetition rate ( $\sim 1/\text{ms}$ ) of the bursts.

## 1 Introduction

Magneto-hydrodynamic (MHD) activity, naturally emerging from magnetically resonant regions where the rotational transform is a low-order rational value, is ubiquitous in toroidal magnetic confinement plasmas. In addition, these plasmas show characteristic MHD activities related with specific confinement states where more or less coherent modes are involved. Among many examples we can cite [1, 2, 3, 4, 5] for tokamak and [6, 7, 8, 9] for helical devices. It can be said that, aside from well-known detrimental effects, magnetic resonances can become beneficial external controllers, e.g. for the onset of internal transport barriers [10], ELM mitigation via resonant magnetic perturbations (RMP) [11] or the concept of island divertors [12].

The experience concerning MHD activity and transport quality in the TJ-II heliac is quite ample owing to its design characteristics. General MHD activity in relation with improved confinement is known from the initial experiments [13]. It has been confirmed that rational surfaces are at the origin of macroscopic transport events such as particle bursts, internal crashes and transport barriers [14]; and causality experiments have proven that a proper placement of magnetic resonances inside the plasma favours the formation or destruction of transport barriers [15]. The latter do not necessarily form right at the plasma edge, which is the reason why the quality of H-mode in the TJ-II depends

sensitively on magnetic configuration [16]. Finally, dynamical pre-transition states with pronounced oscillations in the plasma rotation resembling limit cycles require the presence of low order magnetic resonances inside the plasma [17]. Here we show how island rotation dynamics is involved in confinement states associated to the development and stability of transport barriers in the plasma column.

## 2 Confinement states and associated MHD activity

### 2.1 Steady and unsteady island rotation

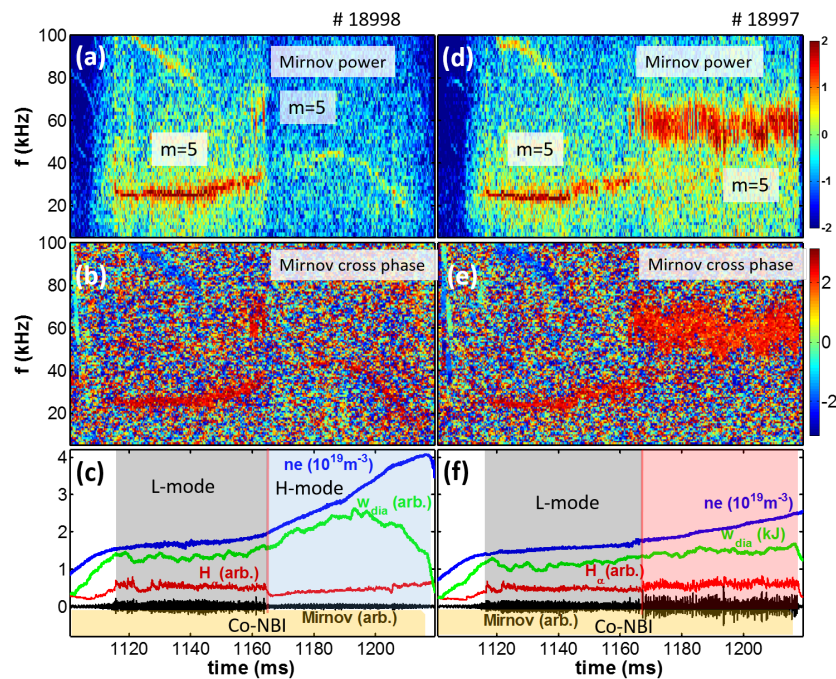


Figure 1: TJ-II discharges #18998 (a-c) and #18997 (d-f). (a)&(d) Cross-power and (b)&(e) cross-phase spectrograms of Mirnov coil signals; (c)&(f) line average density  $\bar{n}_e$ , diamagnetic energy  $W_{\text{dia}}$ ,  $H_\alpha$  signal, and magnetic fluctuations ( $5 \leq f \leq 100$  kHz). Shading indicates plasma in L-mode (grey), H-mode (blue) or a threshold state (pink) characterized by bursting modes (see also figure 2).

Island rotation modes have frequencies generally below 100 kHz in both ECRH (central values  $n_{e0} \sim 0.6\text{--}1.0 \times 10^{19} \text{ m}^{-3}$ ,  $T_{e0} \sim 1$  keV) and NBI ( $1\text{--}5 \times 10^{19} \text{ m}^{-3}$ , 0.3 keV) plasmas. When the wall conditioning allows for a sustained NBI plasma, it is common that confinement transitions are produced with the creation of transport barriers in the outer half, i.e.  $0.5 < \rho = r/a < 0.9$  in normalized cylinder-like radius depending on magnetic configuration. The process is often unstable in the sense that such barriers break and re-establish in a cyclic manner, resembling ELM activity with typical  $\sim 1$  ms

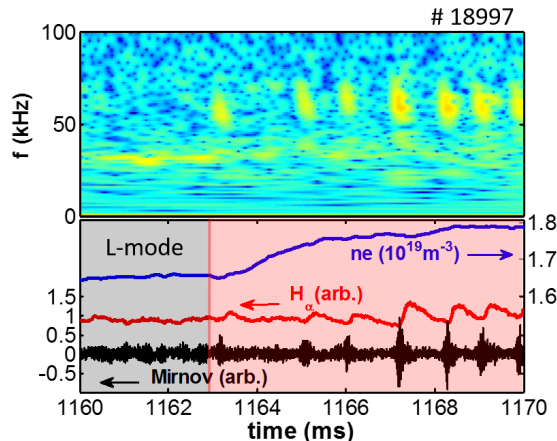


Figure 2: (a) Detail of figure 1 (f) around the establishment of the bursting mode, where its chirping nature can be appreciated in correlation with  $H_\alpha$  pulses.

repetition rates [14, 18], smaller than global  $\sim 10$  ms confinement times. Poloidal mode number analyses [19] show the relation between these modes and magnetic resonances forming islands in the region. Many of these aspects are illustrated in figure 1. Stable rotation can be found in L-mode plasmas, see panels (a)–(c), characterized by peaked density profiles. The mode frequency is  $\sim 30$  kHz in this case with associated  $m = 5$  poloidal mode number. The time traces of line electron density, diamagnetic energy and  $H_\alpha$  light intensity are rather constant in coincidence with a noisy magnetic activity. When the plasma enters H-mode, the rotation speed tends to increase but the mode dims noticeably or becomes undetectable. The cross-phase analysis indicates that the new mode, now around 40 kHz ( $1170 < t < 1190$  ms) corresponds to the same poloidal number. Panels (d)–(f) in figure 1 correspond to a very similar discharge except that the average density in the initial L-mode phase is slightly smaller. However, instead of entering H-mode, the plasma remains in a different state characterized by unstable rotation with chirping-down frequencies. From the cross-phase in panel (e) we deduce that this unstable mode still corresponds to the same  $m = 5$  mode despite the fact that the frequency doubles in a short time ( $< 1$  ms). The diamagnetic energy stays slightly above L-mode but clearly below H-mode according to the previous discharge in the same operation conditions. Observe in figure 1(c) that this kind of bursting mode happens also for a short time, around  $t = 1160$  ms, at the L-H transition threshold.

Figure 2 is a zoom into figure 1(f) focusing on the transition from stable to unstable island rotation. Here we see its characteristic chirping-down nature and its relation with confinement: depending on the amplitude of magnetic bursts and the time interval between them, the  $H_\alpha$  bursts also change amplitude and the average density follows accordingly. Therefore we find that this state of unstable island rotation, which can nonetheless remain for a long time, happens at the threshold condition for the known formation of transport barriers around resonant locations [14, 15].

The interpretation of the modes as island rotation is based on routine knowledge

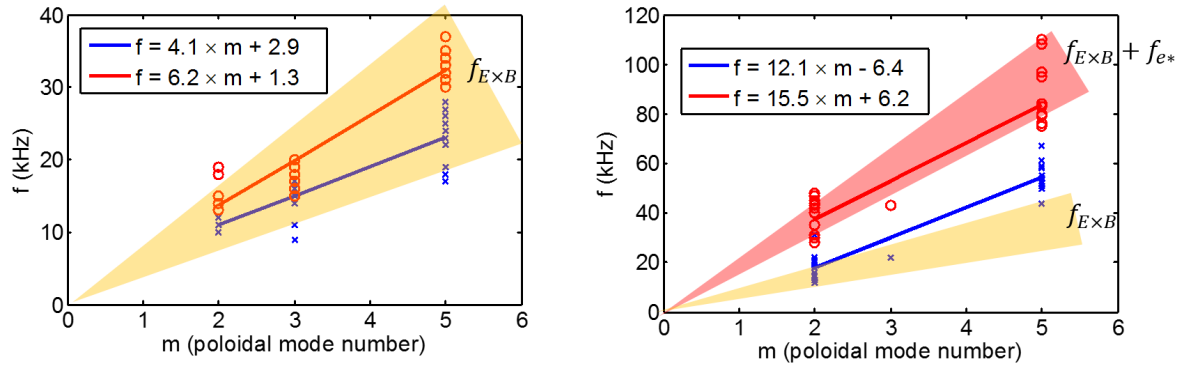


Figure 3: (a) Frequency scaling with poloidal mode number in  $L$ -mode plasma during NBI heating. The shaded area covers values expected from  $E \times B$  rotation. (b) Same plot for the bursting chirping mode. Fits are shown for the highest (circles) and lowest (crosses) frequencies covered by the chirping. Coloured shading indicate the frequency ranges expected from  $u_E$  or  $u_E + u_{*e}$  velocities.

about the vacuum rotational transform and its modifications based on measured net plasma current and estimated non-inductive contributions to the current (NBI-driven and bootstrap). Generally speaking, the displacement of the vacuum location of low order rationals is quite small when the latter locate in  $\rho \gtrsim 0.5$ . When detectable, the poloidal mode numbers  $m$  systematically coincide with the expected low order rationals according to the magnetic configuration, like  $\iota = 8/5$  in figure 1. This information is used in figure 3 to plot the measured frequencies as a function of  $m$ . In figure 3 (a), blue crosses and red circles represent respectively lower and upper frequencies due to variations in rational surface position and plasma profiles for each discharge. The corresponding linear fits are shown separately. The shaded region covers the expected mode frequencies if they were due to the rotation of islands with the indicated  $m$  and locked in the frame moving with  $E \times B$  velocity, often called “plasma frame”; i.e., in the shaded region  $f = m u_E / 2\pi r$  where  $u_E$ , or magnitude of the  $\mathbf{E} \times \mathbf{B} / B^2$  velocity, is taken in the range 3–6 km/s as found in NBI heated plasma with line average densities near  $2 \times 10^{19} \text{ m}^{-3}$  [16]. The phase analysis shows that the magnetic perturbations propagate in the electron diamagnetic direction, as expected from the all-negative radial electric fields characteristic of these plasmas [20, 21]. Additionally, in lower density plasmas where Electron Cyclotron Emission (ECE) still emerge, channels at both sides of the resonant location are modulated at the rotation frequency but in phase opposition, as expected from the modulation of the electron temperature due to the rotating island chain.

In figure 3 (b), the bursty-mode frequency is also plotted against  $m$ . Since the modes frequency is chirping down or quite changeable, we split again the data in upper (circles) and lower (crosses) frequencies and perform separate linear fits. The two shaded regions cover frequencies calculated as  $f = m u / 2\pi r$  assuming that an  $\iota = n/m$  island rotates due to some drift velocity  $u$  at position  $\rho = 0.7$ . In the lower shaded region, we assume island movement within  $u_E$  velocity range, which is estimated 5–8 km/s. The upper shaded

region assumes  $u_E$  plus electron diamagnetic frequency taking a fixed  $u_E = 7$  km/s and the electron diamagnetic velocity  $u_{*e}$  in the range 7–11 km/s, which corresponds to  $0.7 < \rho < 0.9$  in these plasmas depending on local density gradient length. The interest of doing so is to show that, recalling the plasma frame as that locally moving with the electric drift  $u_E$ , upper frequencies match the electron drift frequency while the lower ones still have some speed (i.e., they lie above the frequencies expected from  $E \times B$  drift in the laboratory frame). The chirping-down frequency indicates that, in the plasma frame, the islands start drifting with practically the diamagnetic speed but tend to stop as the plasma evolves during the short duration of each chirp.

The basic phenomenology shown in figure 1, namely, (i) the approximately stable island rotation in L-mode, (ii) the same rotation considerably dimmed or non detectable after a stable transport barrier is established; and, finally, (iii) the unstable rotation in an intermediate threshold state, is found in many hundreds of TJ-II discharges. Next examples are intended to provide more detail on the intermediate threshold state based on diagnostic availability.

## 2.2 The relation between unstable rotation mode and transport barrier dynamics

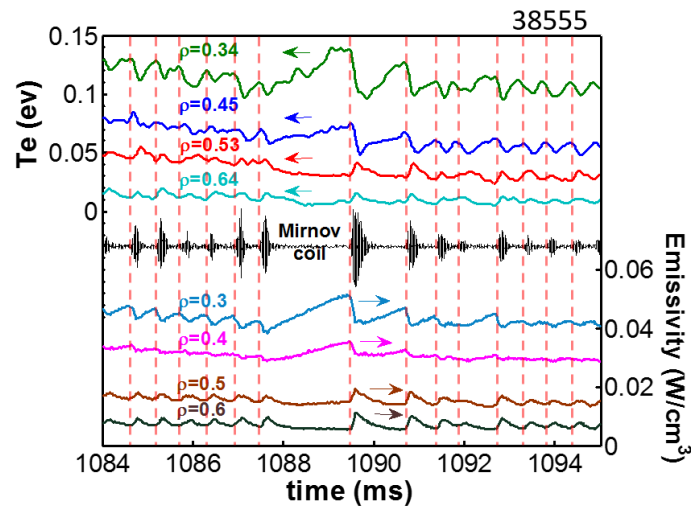


Figure 4: TJ-II discharge #38555. Time evolution of the electron temperature and radiation emissivities from different radii (labelled) showing the existence of a pivot point around  $\rho = 0.5$ ; and band-pass filtered ( $5 \text{ kHz} \leq f \leq 100 \text{ kHz}$ ) Mirnov-coil signal.

Pivot points that show barrier breaking around resonant locations during the phase of bursting chirping mode were already identified in TJ-II NBI plasmas [14], but not their relation with magnetic island rotation modes. Figure 4 shows a detail of the evolution of local electron temperatures and radiation emissivities during the bursty mode activity in

discharge #38555 with  $\tau = 3/2$  at  $\rho \approx 0.5$ . The time window corresponds to a short (10 ms) constant density period  $\bar{n}_e = 0.8 \times 10^{19} \text{ m}^{-3}$ . The chirping consists of a repetition of individual MHD events, starting at each vertical line, that are best appreciated when their amplitude is large. A pivot radial point,  $\rho_p$ , is clearly deduced from both signals, temperature and radiation. Preceding the burst there is a quiescent phase during which  $T_e$  increases for  $\rho < \rho_p < 0.5$  but tends to decrease for  $\rho > \rho_p$ , an obvious expectation for a transport barrier at  $\rho_p$  with most of the heat source inside. The barrier is broken in a very fast time-scale, in view of the sudden change of tendency starting at each vertical line:  $T_e(\rho < \rho_p)$  drops sharply while it increases for  $\rho > \rho_p$ . Then the chirping starts from a high frequency ( $\approx 60 \text{ kHz}$ , similar to the case in figures 1(d)–(f)) growing in amplitude for some  $100 \mu\text{s}$  and then decaying in around  $300 \mu\text{s}$  (not resolved in this figure). Observe that when this decay starts, the barrier gets re-established:  $T_e(\rho < \rho_p)$  increase again while they decrease outside  $\rho_p$ . Similar information is obtained from the reconstructed radiation emissivities, which confirm the existence of a pivot point  $\rho_p \lesssim 0.5$ .

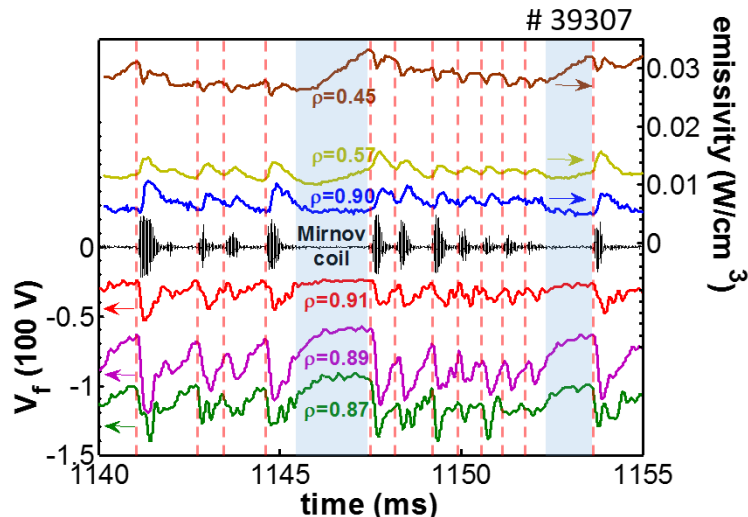


Figure 5: Discharge #39307 with  $\tau = 3/2$  around  $\rho = 0.5$ . Time traces of: radiation emissivities from the indicated radii, Mirnov-coil signal ( $5 \text{ kHz} \leq f \leq 100 \text{ kHz}$  frequency band) and  $V_{\text{fl}}$  from Langmuir probes at  $\rho = 0.91$ ,  $\rho = 0.89$  and  $\rho = 0.87$ .

Regarding the edge, where ECE measurements are not possible in the TJ-II, we have selected a discharge where floating potential,  $V_{\text{fl}}$ , measurements are available from electric probes.  $V_{\text{fl}}$  can illustrate with good time-resolution the arrival of transport pulses to the edge because it is sensitive to plasma potential and electron temperature. In figure 5 we show data from discharge #39307, operated in a magnetic configuration where  $\tau = 3/2$  is located around mid-radius. Low-pass filtered (10 kHz)  $V_{\text{fl}}$  signals from a multi-pin electric probe [22] are shown for pins inserted at three nearby radial locations, along with a magnetic signal. The emissivities from several radii are also plotted to establish a clear link between the MHD events originated around the resonant location (here  $0.45 < \rho_p < 0.57$ ) and the probe signals. In particular, note how  $V_{\text{fl}}(\rho = 0.91)$  mirrors the emissivity from

$\rho = 0.90$  (the same happens with other radial locations), a clear indication that  $V_{\text{fl}}$  is contributed by  $T_e$ . During the short quiescent MHD periods with transport barrier (we highlight the longest ones with shading) the edge plasma shows an increment of  $V_{\text{fl}}$  up to eventual saturation.  $V_{\text{fl}}$  undergoes a sudden drop in coincidence with barrier collapse and consequent bursting chirping mode. Vertical dashed lines indicate the instants when the innermost probe ( $\rho = 0.87$ ) starts dropping, so we can appreciate that outer probes are slightly delayed as expected from outwards propagation.

### 3 Discussion and conclusions

Two rotation states have been identified: stable rotation scaling like the ExB drift and unstable rotation with an added diamagnetic drift (figure 3). Stable rotation is compatible with stable L- or H-mode states. Around the resonant regions of the surveyed plasmas, the parameter [23]  $C = (L_s/L_n)^2(\nu_e/\omega_{*e})m_e/m_i \lesssim 1$  despite the large magnetic shear length  $L_s$  in TJ-II configurations. Here  $L_n$  is the density gradient length and  $\nu_e$  is electron collisionality. It is then reasonable to expect that the width  $W$  of our island chains is on the order of, or larger than, the ion sound Larmor radius ( $\sim 2$  mm around the resonant locations here studied) corrected by this factor, i.e.  $W > \rho_s\sqrt{C}$ . In these conditions the islands are expected to rotate with the ExB drift. Faster ExB drifts related with the steepening of plasma profiles can enhance magnetic screening and island shrinking [24] during the H-mode, thus explaining why the rotation modes are strongly weakened despite the larger rotation speeds (figure 1 (a)). The unstable rotation that provokes bursting-chirping modes happens because the formation of transport barriers in the vicinity of magnetically resonant regions can render the latter unstable. We conjecture that, when the barrier resists, the resonant layer is thin; when it breaks, transport flows cross rapidly this layer and establish a density gradient there. The islands structure grows again (increasing coherent magnetic fluctuations) in an environment where the rotation approaches the diamagnetic drift in the ExB frame [23]. A rapid relaxation of the density gradient in the resonant layer provokes the rapid frequency chirping-down while the local conditions for MHD instability are abandoned, so a barrier can form again. Owing to continuous energy supply in the centre, the gradients build up anew and the cycle restarts. Unfortunately, we do not have enough spatio-temporal resolution to distinguish local density flattening in the resonant locations. This bursting-chirping mode is a sustained threshold state because it consists of a repeated destruction and creation of transport barriers around rational surfaces; and its confinement quality depends on the repetition rates. We have also noted that, even when the corresponding rational surfaces are well inside the plasma, the barrier destruction can cause detectable pulses of particles and heat all the way to the edge. We encourage corresponding studies (e.g. [25]) due to their potential impact on H-mode control via RMPs, as in axisymmetric devices, or whatever means of rotational transform control in current-less devices.

**Acknowledgement:** This work has received funds from the Spanish government via project Ref. ENE2014-52174-P.

## References

- [1] GREENWALD M., et al., Phys. Plasmas **6** (1999) 1943-1949.
- [2] BURRELL, K. H., et al., Plasma Phys. Control. Fusion **44** (2002) A253.
- [3] PEREZ, C. P., et al., Plasma Phys. Control. Fusion **46** (2004) 61.
- [4] HUBBARD, A. E., et al., Phys. Plasmas **18** (2011) 056115.
- [5] OSBORNE, T. H., et al., Nucl. Fusion **55** (2015) 063018.
- [6] WELLER, A., et al., Phys. Plasmas (1994-present) **8** (2001) 931-956.
- [7] MORITA, S., et al., Plasma Phys. Control. Fusion **48** (2006) A269.
- [8] TOI, K., et al., Plasma Phys. Control. Fusion **48** (2006) A295.
- [9] SAKAKIBARA, S., et al., Plasma Phys. Control. Fusion **50** (2008) 124014.
- [10] CONNOR, J. W., et al., Nucl. Fusion **44** (2004) R1.
- [11] EVANS, T. E., et al., Nucl. Fusion **48** (2008) 024002.
- [12] FENG, Y., et al., Nucl. Fusion **46** (2006) 807.
- [13] GARCÍA-CORTÉS, I., et al., Plasma Phys. Control. Fusion **44** (2002) 1639–1649
- [14] LÓPEZ-BRUNA, D., et al., Nucl. Fusion **53** (2013) 073051.
- [15] LÓPEZ-BRUNA, D., et al., Plasma Phys. Control. Fusion **53** (2011) 124022.
- [16] ESTRADA, T., et al., Contrib. Plasma Phys. **50** (2010) 501–506.
- [17] ESTRADA, T., et al., Nucl. Fusion **55** (2015) 063005.
- [18] ESTRADA, T., et al., Plasma Phys. Control. Fusion **51** (2009) 124015.
- [19] JIMÉNEZ-GÓMEZ, R., et al., Nucl. Fusion **51** (2011) 033001.
- [20] VELASCO, J. L., CASTEJÓN, F., Plasma Phys. Control. Fusion **54** (2012) 015005.
- [21] GUTIÉRREZ-TAPIA, C., et al., Plasma Phys. Control. Fusion **57** (2015) 115004.
- [22] PEDROSA, M. A., et al., Nucl. Fusion **51** (2011) 073027.
- [23] WAELBROECK, F. L., Nucl. Fusion **49** (2009) 104025.
- [24] NARUSHIMA, Y., et al., Nucl. Fusion **51** (2011) 083030.
- [25] WAELBROECK, F. L., JOSEPH, I., NARDON, E., BÉCOULET, M., FITZPATRICK, R., Nucl. Fusion **52** (2012) 074004.